Published in final edited form as:

J Immunol. 2008 November 15; 181(10): 6872–6881.

Antiviral Activated Dendritic Cells: A Paracrine Induced Response State[1]

Antonio V. Bordería[#*], **Boris M. Hartmann**[#†], **Ana Fernandez-Sesma**[*], **Thomas M. Moran**[*], and **Stuart C. Sealfon**[†,‡]

[*]Department of Microbiology, Mount Sinai School of Medicine, New York, NY.

[†]Department of Neurology, Mount Sinai School of Medicine, New York, NY.

[‡]Center for Translational Systems Biology, Mount Sinai School of Medicine, New York, NY.

[#] These authors contributed equally to this work.

Abstract

Infection of immature dendritic cells (DCs) by virus stimulates their maturation into antigen presenting cells (APC). Infected DCs can also expose uninfected DCs to a panoply of cytokines/chemokines via paracrine signaling. Mathematical modeling suggests that a high rate of paracrine signaling is likely to occur among DCs located in three-dimensional space. Relatively little is known about how secreted factors modify the early response to virus infection. We used a trans-well experimental system that allows passage of secreted factors, but not direct contact, between virus-infected DCs and uninfected DCs to investigate paracrine signaling responses. Paracrine signaling from infected DCs induced an antiviral-primed DC state distinct from that of mature virus-infected DCs that we refer to as antiviral activated DCs (AVDCs). AVDCs had increased surface MHC-II and CD86 levels, but in contrast to virus-infected DCs, their MHC-I levels were unchanged. Imaging flow-cytometry showed that AVDCs had an increased rate of phagocytosis compared with naïve DCs. Experiments with IFNβ cytokine indicated that it may be responsible for CD86, but not MHC-II regulation, in AVDCs. Both interferon-inducible and interferon-independent genes are up-regulated in AVDCs. Notably, AVDCs are relatively resistant to virus infection in comparison with naïve DCs and achieve accelerated and augmented levels of co-stimulatory molecule expression with virus infection. AVDCs show a distinct antiviral-primed state of DC maturation mediated by DC paracrine signaling. While further *in vivo* study is needed, the characteristics of the AVDC suggest that it is well-suited to play a role in the early innate-adaptive transition of the immune system.

Keywords

Human; innate immunity; adaptive immunity; infection; viral; maturation

[1]This work was supported by contract HHSN266200500021C and grant U19 AI06231 from the National Institute of Allergy and Infectious Diseases.

Introduction

Dendritic cells (DC) are recognized as a key bridge between the innate and adaptive immune responses (1). A key event in the development of adaptive immunity upon exposure to infection is the maturation of DCs into antigen presenting cells that instruct lymphocytes to generate responses to specific antigens. Activated DCs efficiently stimulate both innate immune cells, including natural killer (NK) cells (2) and natural killer T (NKT) cells (3) as well as key components of adaptive immunity including naïve (4) and memory (5) B cells, and T cells (1). Thus, DCs are important both for innate immunity as well as for various elements of adaptive immunity (6).

Our study focuses on DC activation by virus infection, using Newcastle's Disease Virus (NDV), an RNA paramyxovirus that has been demonstrated to be a good model for immune activation (7). DC maturation is stimulated by detection of various pathogen-associated molecular patterns (PAMPs, (1)) that are characteristic of bacteria, fungi, protozoa or viruses. DCs recognize virus infection either by Toll-like receptors (TLRs) or by TLR independent intracellular viral product detectors such as RIG-I (8) and/or MDA5 (9, 10). Virus recognition activates a signaling cascade involving different cellular factors (IRF3, NFκB, c-jun), causing the expression of type I interferons (IFN) and other inflammatory response genes including TNFα and IL6. The first type I IFN to be produced and secreted is IFNβ (11), which signals either in an autocrine or paracrine manner through the IFN receptor (IFNAR) and activates the JAK-STAT pathway (12). This signaling cascade further amplifies the initial response and creates an antiviral state in adjacent cells that renders them resistant to infection.

Maturation is a complex process, which includes changes in morphology, loss of endocytic/phagocytic receptors, up regulation of co-stimulatory molecules, such as CD86, translocation of MHC compartments to the surface and secretion of cytokines and chemokines (13) that attract, differentiate and polarize other immune effector cells (6). Secretion of chemokines occurs in coordinated waves according to the type of immune cells that need to be attracted and activated (13). One late component associated with maturation is the migration of the DCs to the secondary lymphoid organs (14), where they interact with the naïve T and B cells. This activation of antigen specific T-cells by mature DCs is a major aspect of the initiation of adaptive immunity.

The secretion of the different cytokines and chemokines affects other immune cells, including immature DCs, by paracrine signaling. Consequently, some DCs might be exposed to both cytokines and microbial products (11), whereas others only to inflammatory cytokines. Autocrine signaling is regarded as an important mechanism for virus triggered DC maturation. Integrodifferential modeling of interferon trajectories suggests that about 3% of IFNβ interacts with the DC that produced it (15).

We investigated the effects of paracrine signaling by DCs on the response state of DCs that are not infected by virus, using NDV which is detected primarily through the cytosolic RIG-I molecule (16). To study paracrine effects, we used a trans-well system which is composed of two chambers, separated by a membrane that allows soluble components such as

cytokines and chemokines to diffuse between chambers, but prohibits direct contact between the cells placed in different chambers. DCs infected with NDV and naive non-infected DCs were placed in the upper and lower chamber respectively. The culture was left for 18 hours, allowing the infected DCs to initiate cytokine and chemokine secretion. We found that the naïve DCs exposed to the specific cytokine/chemokine secretions released by infected DCs enter a partially activated state in which they are relatively resistant to virus infection and primed to generate a more rapid and enhanced response to virus infection.

Materials and Methods

Differentiation of DCs

All human research protocols for this work have been reviewed and approved by the IRB of the Mount Sinai School of Medicine. Monocyte-derived DCs were obtained from healthy human blood donors following a standard protocol described elsewhere (7). All experiments were replicated using cells obtained from different donors. Briefly, human peripheral blood mononuclear cells were isolated from buffy coats by Ficoll density gradient centrifugation (Histopaque, Sigma Aldrich, St. Louis, MO) at 1450 r.p.m. and CD14+ monocytes were immunomagnetically purified by using a MACS CD14 isolation kit (Miltenyi Biotech, Bergisch Gladbach Germany). Monocytes were then differentiated into naïve DCs by 5–6 day incubation at 37°C and 5% CO_2 in DC growth media, which contains RPMI Medium 1640 (Invitrogen/Gibco, Carlsbad CA) supplemented with 10% fetal calf serum (Hyclone, Logan UT), 2 mM of l-glutamine, 100 U/ml penicillin and 100 g/ml streptomycin (Pen/Strep) (Invitrogen, Carlsbad CA), 500 U/ml hGM-CSF (Preprotech, Rocky Hill NJ) and 1000 U/ml hIL-4 (Preprotech, Rocky Hill NJ).

Virus preparation and viral infection

The recombinant Hitchner strain of Newcastle disease virus (rNDV/B1) and NDV-GFP were generated in Prof. Peter Palese's laboratory (17, 18) and grown in 9 day embryonated chicken eggs as described previously (17). Recombinant NDV-RFP was obtained from Prof. Adolfo Garcia-Sastre's laboratory (19) and grown and titrated similarly to NDV/B1 and NDV-GFP. NDV viruses were titrated by immunofluorescence 18 hours after infection of Vero cell plates using monoclonal antibodies specific for NDV-HN protein generated by the Mount Sinai Hybridoma Core Facility followed by addition of anti-mouse IgG-FITC and visualization using fluorescent microscopy. For infection of naïve DCs, NDV stocks were appropriately diluted in Dulbecco's Modified Eagle Medium (DMEM) and added directly into pelleted DCs at a multiplicity of infection (MOI) of 1 (7, 20). After incubation for 40 minutes at 37°C, fresh DC growth medium (without GMCSF and IL-4) was added back to the infected cells (1×10^6 cells/ml) for the remainder of the infection. Naïve non-infected DCs underwent the same experimental procedure as infected DCs in the absence of virus to ensure that mechanical manipulations could not be responsible for differences in experimental readouts.

Generation of AVDCs

Antiviral activated dendritic cells (AVDCs) were generated by employing a trans-well system. The trans-well system consists of an upper and a lower chamber separated by a 0.4

μm PET membrane (Millipore) that allows diffusion of cytokines and chemokines through the membrane but avoids the interaction of the cells in both chambers. To generate the AVDCs, naïve DCs were infected as described above. After the 40 minutes incubation, the cells were washed with PBS, and cultured in the trans-well system. Infected and non-infected DCs were allocated in the upper and lower chamber respectively. Two independent wells were set-up with infected or naïve non-infected DCs as positive and negative controls. The cultures were incubated at 37°C in 5% CO_2 for 18 hours. All cells were then washed in PBS and harvested for flow cytometry analysis and RNA isolation. The supernatant was kept at −20°C for ELISA analysis of cytokines/chemokines.

Proteinase K treatment

Supernatants derived from NDV-infected DCs for 18 hours were treated with Proteinase K (MP Biomedicals, CA) for 2 hours at 37°C to digest cytokines and chemokines. The proteinase K was then inactivated with a brief heat treatment. Proteinase K treated and non-treated supernatants were placed in the upper compartment of the trans-well system with naive DCs in the lower compartment to mimic the condition during AVDC generation. We incubated for 18 hours at 37°C. Naïve DCs in the lower compartment were then stained for the maturation markers MHC-I, MHC-II and CD86.

Culture of human lung fibroblast

Lung epithelial fibroblasts were obtained from Lonza (Basel, Switzerland) and cultured according to supplier's instructions. Briefly, cells were passed when confluence was 70-80% using Fibroblast Basal Medium (FBM) media supplemented with hFGFβ, insulin, FBS and gentamicin/amphotericin-B. To perform experiments in the trans-well system, 3×10^5 cells were seeded 8 hours before treatment in the trans-well system with DC media and left at 37°C in the incubator. Fibroblasts were infected with NDV at a MOI of 1 and left in the incubator for 40 minutes. Cells were then washed with PBS and fresh DC media was added to the culture. Naïve DCs were added in the upper compartment and left the trans-well system for 18 hours in the incubator.

IFNβ treatment

DCs were generated as described previously, and IFNβ (PBL Interferon Source, Piscataway,NJ) added to the culture in a concentration of 2000 units/ml. The culture was left for 18 hours in incubation as described before. After the incubation, the cells were washed with PBS and harvested for flow cytometry analysis.

Quantitative RT PCR

Viral and host RNA expression levels were quantified by real-time reverse transcriptase polymerase chain reaction (PCR). RNA was isolated from cells using Qiagen Micro RNeasy kit following the manufactures protocol (QIAGEN, Duesseldorf Germany). cDNA was synthesized from total RNA with AffinityScript™ Multi-Temp RT (Stratagene, La Jolla CA) with oligo dT_{18} as primer. For real-time PCR PlatinumTaq DNA polymerase (Invitrogen, Carlsbad CA) and a SYBR green (Molecular Probes, Carlsbad CA) containing buffer were used. The real-time PCRs were performed using a thermocycler (ABI7900HT; Applied

Biosystems, Foster City, CA) as previously described (21). The RNA levels for the house keeping genes ribosomal protein S11 (*Rps11*), tubulin (*Tuba*), and β-actin (*Actb*) were also assayed in all samples to be used as an internal controls. mRNA measurements were normalized using a robust global normalization algorithm. All control crossing threshold (Ct) values were corrected by the median difference in all samples from *Actb*. All samples were then normalized by the difference from the median Ct of the 3 corrected control gene Ct levels in each sample, with the value converted to a nominal copy number per cell by assuming 2500 *Actb* mRNA molecules per cell and an amplification efficiency of 93% for all reactions. The primer sequences used for the assays were: *NDV-HN* sense: 5′-GAC AAT GCT TGA TGG TGAA C-3′, antisense: 5′-CAA TGC TGA GAC AAT AGG TC-3′; *NDV-NP* sense: 5′-GGC TAT GGT CAC AGA GAG ACA C-3′, antisense: 5′- CAA TTA TTG CTG GCG GTG GCA C-3′; *IFNβ* sense: 5′- GTC AGA GTG GAA ATC CTA AG -3′, antisense: 5′- ACA GCA TCT GCT GGT TGA AG -3′; *IFNα1* sense: 5′- CTG AAT GAC TTG GAA GCC TG-3′, antisense: 5′-ATT TCT GCT CTG ACA ACC TC-3′; *PKR* sense: 5′-TTG TAC CAC AAG AGA GAG TG-3′, antisense: 5′-AGT GCT GTC CCT CAA GAC TC-3′; *OAS-1* sense: 5′-TTT GAT GCC CTG GGT CAG TT-3′, antisense: 5'-GTG CTT GAC TAG GCG GAT GA-3′; *TNFα* sense: 5′- GAG GAA GGC CTA AGG TCC AC-3′, antisense: 5′- AGT GAA GTG CTG GCA ACC AC-3′; *RIG-I* sense: 5′- AAA GCC TTG GCA TGT TAC AC -3′, antisense: 5′-GGC TTG GGA TGT GGT CTA CT -3′; *Rantes* sense: 5′- AAG CTC CTG TGA GGG GTT GA -3′, antisense: 5′- TTG CCA GGG CTC TGT GAC CA -3′; *IL-6* sense: 5′- CTG AGG TGC CCA TGC TAC AT-3′, antisense: 5′-AAT GCC AGC CTG CTG ACG AA′; *IP-10* sense: 5′-TCC CAT CAC TTC CCT ACA TG-3′, antisense: 5′-TGA AGC AGG GTC AGA ACA TC-3′; *MXA* sense: 5′-CGT GGT GAT TTA GCA GGA AG-3′, antisense: 5′- TGC AAG GTG GAG CGA TTC TG -3′; *Rps11* sense: 5′-CGA GGG CACC TAC ATA GAC A-3′, antisense: 5′-GAG ATA GTC CCG GCG GAT GA-3′; *Actb* sense: 5′-GCC TCA ACA CCT CAA ACC AC-3′, antisense: 5′-CCA CAG CTG AGA GGG AAA TC-3′; *Tuba* sense: 5′-AGC GCC CAA CCT ACA CTA AC-3′, antisense: 5′-GGG AAG TG G ATG CGA GGG TA-3′.

Flow cytometry analysis

Cells were fixed with 1.5% paraformaldehyde (SIGMA), washed with FACS staining buffer (Beckman Coulter) and stained with monoclonal antibodies for MHC-I, MHC-II, CD86. NDV-GFP or NDV-RFP infected cells were stained with antibodies for MHC-I, MHC-II and CD86 (Beckman Coulter, Fullerton CA). Cells were assayed on an LSRII flow cytometer (Beckman Coulter, Fullerton CA) and data was analyzed with the FlowJO software (Treestar, Ashland, OR). To provide higher throughput and reduce cell requirements per assay, we used a modified barcoding method previously described by Nolan *et al* (22). Briefly cells were fixed, then stained in DMSO containing different combinations of 0, 0.3, 1, 4 or 15 μg/ml Pacific Blue–NHS, 0, 1.25, 5 or 20 μg/ml Alexa 350–NHS and 0, 4 or 20 μg/ml Alexa 750–NHS for 15 min at 20–25°C (see Figure 9a). Fluorescence minus one (FL-1) controls were obtained by staining naïve DCs with all fluorochromes studied excluding the fluorochrome of interest, conjugated antibody against CD45 (23).

Imaging flow cytometry analysis of phagocytosis and morphology

Imaging flow cytometry was used to compare the morphology and phagocytosis levels of AVDCs and naïve DCs. To detect phagocytosis, 1 μm 488 nm fluorescence labeled latex microspheres (Polysciences Corp, Warrington PA) at a concentration of 50 beads per cell were co-cultured for 2 hours at 37°C with each celltype. Single cell images were acquired using extended depth field imaging distortion in order to identify beads in different focal planes within a cell. The numbers of beads incorporated by cells were quantified in the images captured using image analysis software (IDEAS software, Amnis Corp, Seattle WA). The distributions were compared using the Kolmogorov Smirnoff technique.

To measure the cellular morphology, AVDCs, naïve DCs and infected DCs were labeled with a live membrane dye, Benzoxazolium, 3-octadecyl-2-[3-(3-octadecyl-2(3H)-benzoxazolylidene) -1-propenyl]-, perchlorate (DiO), following the manufacturer's protocol (Invitrogen). Samples were then individually acquired by imaging flow cytometry. To analyze the morphology, an algorithm described by Haralick *et al* (24) which describes the homogeneity of an given image was used (IDEAS software, Amnis, Seattle WA).

Multiplex ELISA

Four different cytokines/chemokines (IL6, IP10, TNFα and IFNα) concentrations were assayed in the culture media. In order to minimize the supernatant volume to assay, a Beadlyte Human Multiplex ELISA analysis (Millipore) was used following manufacturer instructions. Briefly, 100ul from each compartment/well was incubated in a 96-well filter PVDF 1.2μm plate specially designed to retain cytokines/chemokines, with a mixture of anti-cytokine IgG conjugated beads for the different cytokines/chemokines assayed. After two hours incubation, the plate was filtered and washed three times with Assay solution (PBS pH 7.4 containing 1% BSA, 0.05% Tween-20 and 0.05% sodium azide). The washes were followed by one hour and half incubation with biotin-conjugated anti-cytokine IgG. After Assay solution washing, Streptavidin-Phycoerythrin, was added followed by addition after 30 minutes of Stop solution (0.2% (v/v) formaldehyde in PBS pH 7.4). The plate was then filtered and each well resuspended in 125μl of Assay buffer, and read in a Luminex 100 machine.

Results

Effectiveness of trans-well chambers to study paracrine signaling

In order to isolate the effects of direct infection by virus from that of paracrine signaling on naïve dendritic cells, we used a trans-well culture system. Naïve, immature DCs were infected with NDV and immediately placed in the upper chamber. Non-infected naïve DCs were placed in the lower chamber. The chambers were partitioned by a 0.4 μm pore membrane that allowed the diffusion of cytokines and chemokines (Figure 1). After incubation, cells in each chamber were recovered and analyzed for their surface marker and gene expression patterns.

DCs do not support the productive infection of NDV (25). To ascertain whether viral particles could infect cells in the lower chamber during these experiments, we performed

control experiments with a recombinant NDV containing a GFP tagged HN protein (17). Infection of cells was assayed by flow cytometry. When NDV-GFP infected cells were incubated in the upper chamber for 18 hours, GFP fluorescence was detected only in cells from the upper, but not the lower chamber, indicating that the experimental system effectively separated infected and uninfected DCs (Figure 2).

As a further test of the isolation of virus infection, the induction of the NDV-HN and NDV-NP viral genes and virus-induced type I IFN genes were compared in membrane-separated co-cultured cells using real-time PCR assays. Both viral genes were present in virus-infected DCs from the upper chamber and were undetectable in non-infected control DCs and in DCs co-incubated in the lower chamber (Figure 3). Viral components lead to activation of type I interferon via toll-like receptor activation. If uninfected cells were exposed to viral components that passed through the membrane, they would be expected to show induction of type I interferons. Therefore we also assayed the expression of IFNβ and IFNα1 as a sensitive assay of exposure to very small amounts of virions, viral RNA, debris or other small particles that might cross the membrane (26). Using a sensitive real-time PCR assay, we found that both IFNs were up regulated in virus-infected DCs from the upper chamber, but were not induced in naïve cells incubated in the lower chamber (Figure 3). The results of flow cytometry and real-time PCR indicate that the culture system completely eliminates direct virus infection of uninfected, membrane-isolated co-cultured cells. In order to test further the possibility that viral components such as RNA caused the surface marker up-regulation pattern observed (see below), we tested the effect of proteinase K digestion of supernatants from infected DCs on its capacity to affect naïve DCs. Proteinase K treated supernatant did not to up-regulate the surface markers of DCs in the other trans-well chamber. Supernatants from infected DCs that were not digested with proteinase K induced a similar surface marker pattern to that seen in AVDCs in the trans-well system (Supplementary Fig. S1). Thus any responses of the uninfected DCs in the lower chamber were the results solely of paracrine signaling initiated by infected DCs in the upper chamber.

Effects of DC paracrine signaling on maturation markers

Several cellular surface proteins have been described as maturation markers of DCs, including CD86, MHC-I and MHC-II (6). There is an increase in the density of these markers in the cellular membrane of the DCs upon activation and maturation. In our co-culture trans-well system, upper chamber infected DCs and the positive controls DC showed a comparable up regulation of MHC-I, MHC-II and CD86 molecules (Figure 2a, c) indicating the maturation of those cells. Interestingly, lower chamber DCs in the co-culture trans-well system also showed an up regulation of MHC-II and CD86 molecules, while MHC-I remained at levels equivalent to the non-infected control DCs levels (Figure 2b).

To determine whether the changes in naïve DCs induced by infected DCs were unique to infected DCs, we studied the effects of secreted factors from NDV-infected primary lung fibroblasts on naïve DCs using the transwell system. Our results showed that the presence of infected primary lung fibroblast instead of infected DCs in the same trans-well system did not induce a comparable surface marker expression pattern in the naïve DCs (Supplementary Fig. S2). Furthermore, non-infected control DCs did not up-regulate any of the surface

markers, even if cells were maintained in the trans-well system for periods up to 48 h (Fig. S2). These results indicate that the experimental manipulations alone were not affecting maturation marker up-regulation. Our results suggest that paracrine signaling alone between infected and uninfected DCs produces an increase of some DC maturation markers leading to a unique DC state that differs both from naïve DCs and from fully matured virus-infected DCs.

Levels of paracrine cytokines

We assayed cytokines that could contribute to paracrine activation of DCs. Factors secreted by DCs for which DCs expressed receptors include IL6, TNFα, IP10 and type I IFN. Measurement of the levels of these cytokines in upper and lower chambers by ELISA during a co-culture experiment indicated high levels of all four cytokines were achieved in the lower chamber (Figure 4).

Gene program response in AVDCs

In order to further understand the characteristics of the paracrine-generated AVDC state, the regulation of a variety of genes was assayed by real time PCR in AVDCs, NDV-infected DCs and naïve DCs. Paracrine and autocrine IFN acting at the type I IFN receptor activates a number of genes through JAK-STAT signaling, including PKR, OAS, MxA and IP10. Consonant with the detection of high levels of IFNα in the medium by cytokine assays (Figure 4), AVDCs showed robust induction of these IFN-activated genes (Figure 5). OAS and MxA showed the same levels in the lower chamber as in infected DCs. While PKR and IP-10 were lower than in infected DCs, they were still significantly induced in comparison with non-infected DCs. IFN is a key paracrine signaling factor during virus infection and has long been recognized to generate complex transcriptional responses (7, 26). However the state of AVDCs appears to result from additional factors besides IFN, because genes such as TNFα, which are not inducible by IFN are up regulated in AVDCs (Figure 5). The hypothesis that additional secreted factors contribute to the AVDC state was further supported by comparing the pattern of maturation markers in AVDCs and in IFNβ treated naïve DCs. The induction of the co-stimulatory molecule CD86 was similar in AVDCs and IFN-exposed DCs, suggesting that this regulatory event may result from IFN signaling. However, the increased expression of MHC-II was seen only in AVDCs (Figure 6). Overall, the gene response patterns and maturation marker analysis indicate that type I IFN signaling represents only part of the paracrine environment necessary for the generation of AVDCs.

Quantification of AVDC morphology and rate of phagocytosis

The morphology of AVDCs and naïve DCs was compared using imaging flow cytometry. Cells were stained with a live-cell membrane-localized dye, DiO, and morphology was measured using the texture analysis algorithm developed by Haralick *et al* (24) as implemented in IDEAS software (see Materials and Methods). By this method, the spatial relationships between the texture features and the pixel values in an image were measured, and an H Homogeneity mean and a standard deviation value were obtained for each set of cells. The H Homogeneity is a measure of the average shape of a cell. Representative raw images are shown in Figure 7a. These analyses reveal that the average morphology of AVDCs is different from that of naïve DCs. AVDCs showed an increase in textural

homogeneity compared with naïve cells that was comparable to the level seen in infected DCs (Figure 7b).

The rates of phagocytosis of naïve DCs and AVDCs were also compared using high resolution imaging flow cytometry. Both cells types were incubated for 2 h with 1 μm 488 nm fluorescence labeled latex microspheres. The number of particles taken up by each cells was quantified in approximately several thousand cells in each group using automated image analysis (Figure 8a). In three independent experiments using cells from different donors, AVDCs showed significantly higher rates of phagocytosis.

AVDCs resist viral infection and showed enhanced generation of maturation markers by infection

We next investigated whether AVDCs differ from naïve DCs in their response to direct virus infection by NDV. For this purpose, AVDCs generated by co-culturing with NDV-GFP infected DCs for 18 h using the trans-well system, and naïve DCs were exposed to a recombinant NDV virus expressing RFP (NDV-RFP, (19). The level of RFP signal generated over 12 hours was assayed by flow cytometry, as a reflection of the generation of intracellular viral protein within the DCs following direct infection. In order to allow accurate comparison of the level of signal in different samples, a bar-coding flow cytometry approach was utilized (22). In this approach each sample was first labeled with a characteristic pattern of three deconvolution dyes (Figure 9A) and then the 60 mixed samples were labeled with fluorescently labeled surface marker antibodies. Detection of virus protein expression and surface marker expression in each sample was then assayed in a single multispectral flow cytometry run. This analysis showed that AVDCs generated much lower levels of viral protein with infection than naive DCs (Figure 9b). These results indicate that, in comparison with naïve DCs, the AVDCs showed a relatively virus-resistant state.

Interestingly, AVDCs also expressed much higher levels of maturation markers than naïve DCs following virus infection. Time course analysis by flow cytometry showed that the levels of CD86, MHC-I and MHC-II were dramatically higher in infected AVDCs at all time points than in infected naïve DCs (Figure 9c). Notably, this enhanced activation state included both the CD86 and MHC-II markers that were increased in AVDCs without infection as well as the MHC-I signal that was unchanged in AVDCs prior to virus infection. These results indicate that the paracrine signaling environment cause the DCs to enter a state in which they are relatively resistant to infection by virus and their maturation response to infection is greatly enhanced.

Discussion

These experiments reveal that paracrine signals from virus-infected cultured human DCs act on naïve uninfected DCs to induce an activated antiviral state. This AVDC state is characterized by basal up-regulation of CD86 and MHCII cell surface markers, induction of a variety of antiviral-response genes, altered morphology and increased basal phagocytosis. The antiviral state of these AVDCs is evident from their relative resistance to virus infection and their enhanced rate and level of maturation marker expression following infection.

These features of the AVDC are well-suited to facilitate the development of adaptive immunity to virus infection.

The trans-well experimental system with which we characterized the AVDC, while used in various studies of immune cell differentiation (27), has not previously been utilized to study paracrine signaling among immune cells. The pore size of the PET membranes present in our experiments would not be expected to restrict virus particles or components. NDV does not cause productive viral infection in DCs (24). Nevertheless, we tested whether the trans-well culture system might effectively separate the paracrine stimulated naïve DCs from the effects occurring with direct encounter with virus. Using sensitive assays for expression of fluorescent viral protein and stimulation of virus-infection dependent gene expression (viral proteins and type I IFN induction), we demonstrated that the change in state seen in the AVDC results solely from the transmission of secreted factors, and that AVDCs do not show any signs of infection by the virus or exposure to viral components.

Since the discovery of the effects of type I IFN more than 50 years ago, these cytokines have been well-studied as inducers of a variety of antiviral responses that promote the development of DC maturation (28). We have shown previously that NDV infection of human DCs results in a strong activation pattern, including production of type I IFN, TNFα and other pro-inflammatory cytokines as well as IFN inducible genes (7). We find that NDV-infected DCs, located in the upper chamber of the trans-well system, also secrete TNFα, IL6 and IP10, which have receptors present on DCs and are therefore also potential paracrine factors (See Fig. 4). Several previous studies have considered the role of uninfected or “bystander” DCs in the response to virus infection (28-30). However, the effects of paracrine signaling on these bystander cells has either not been evaluated or attributed entirely to type I IFN. Therefore we were interested in determining the role of type I IFN in generating the AVDC state that we have identified. We found that only some of the characteristics of AVDCs can be attributable to type I IFN signaling, indicating that the state of these cells reflects more complex, multifactor paracrine signals. The identification of which combinations and concentrations of factors are responsible for generating the AVDC state is an interesting subject for further investigation.

Pretreatment of immature DCs and/or DC precursors with single cytokines that are secreted either by DCs or other immune cells has been reported to lead to distinct cellular phenotypes. The effects of type I IFN (31-33), thymic stromal lymphopoietin (TSLP, (34, 35)), TNFα (36), IL10 (37, 38), IFNγ (39) and IL15 (6, 40-42) have all been reported. During infection of a host, the extracellular environment of the DCs in the infected tissue *in vivo* contains multiple cytokines and chemokines and the response state of the uninfected DC is likely to result from more than a single factor. Understanding the mechanisms underlying the effects of the integration of multiple signals has been the object of several experimental and computational systems biology studies (43-45). Recently we have begun to develop models to describe paracrine and autocrine signaling among DCs located in three-dimensional space (15). Understanding the mechanisms by which AVDCs are generated is facilitated by studies integrating mathematical simulation with cytokine interaction studies.

Paracrine and autocrine signaling are recognized to contribute to the maturation of DCs following TLR stimulation (42, 46-49). Roman Spörri and Caetano Reis e Sousa found that paracrine signaling cannot substitute for contact for TLR-mediated contact with pathogen components in generating fully activated DCs (49). To our knowledge, the investigation of the role of paracrine signaling in modulating the DC response to subsequent encounter with virus, a sequence likely to occur during actual infection, has not been previously investigated.

During the early stages of infection, only a few cells are infected. In the case of respiratory virus, inhalation of only a few droplets containing virus particles can be sufficient to induce a successful infection, and virus transmission usually involves few viral particles (50). Thus, early in the infection, only a few DCs are likely to come into contact with virus or with virus infected tissue. Therefore we hypothesize that paracrine signaling events capable of inducing the generation of AVDC are likely to play an important role in the early response stages of the immune system to virus infection (Fig. 10). Infection of primary lung fibroblasts were not able to generate AVDCs (Fig. S2), indicating that the AVDC is not generated by exposure to secreted factors from any cell type. Pathogenic viruses express immune antagonists that prevent the activation of innate immune responses in infected cells (51-53). AVDCs could be able to respond even in the face of a viral antagonist due to their heightened activated state. Results obtained in cultured cells can be extrapolated only cautiously to the intact organism. However characterizing the state of these cells and the mechanisms underlying their induction is important to set the stage for investigating the presence and role of AVDCs using *in vivo* models.

In conclusion, the characteristics of the AVDC suggest that they are in an advanced state of readiness, but also capable to resist the negative effects of the virus infection. In the case of human host viruses, the formation of AVDCs may provide an important process to generate antigen presenting cells capable of overcoming the effect of viral protein inhibitors on the maturation of DCs. AVDCs were relatively resistant to virus infection and showed induction of several genes, including RIG-I, PKR and OAS, that promote virus resistance. More importantly for their proposed role in the transition from innate to adaptive immunity, they showed an accelerated rate of maturation when infected and an increased level of expression of maturation markers needed for productive interaction with T cells. The increased phagocytosis rate and increased morphological texture of AVDCs also make them suitable for heightened antiviral surveillance and response.

Supplementary Material

Refer to Web version on PubMed Central for supplementary material.

Acknowledgements

We thank Mathieu Coppey and Stas Y. Shvartsman, for fruitful discussions. We also would like to thank Gary Nolan for organizing the advanced flow cytometry workshop. We thank Peter Palese, Adolfo Garcia-Sastre and Luis Martinez-Sobrido for generously providing the viral chimeras and Esther Rhee and Nada Marianovič for technical assistance. We thank the Mount Sinai flow cytometry and the Microarray, PCR and Bioinformatics Shared Research Facilities for assistance with these studies.

References

1. Reis e Sousa C. Activation of dendritic cells: translating innate into adaptive immunity. Curr Opin Immunol. 2004; 16:21–25. [PubMed: 14734106]
2. Fernandez NC, Lozier A, Flament C, Ricciardi-Castagnoli P, Bellet D, Suter M, Perricaudet M, Tursz T, Maraskovsky E, Zitvogel L. Dendritic cells directly trigger NK cell functions: cross-talk relevant in innate anti-tumor immune responses in vivo. Nat Med. 1999; 5:405–411. [PubMed: 10202929]
3. Kadowaki N, Antonenko S, Ho S, Rissoan MC, Soumelis V, Porcelli SA, Lanier LL, Liu YJ. Distinct cytokine profiles of neonatal natural killer T cells after expansion with subsets of dendritic cells. J Exp Med. 2001; 193:1221–1226. [PubMed: 11369793]
4. Caux C, Massacrier C, Vanbervliet B, Dubois B, Durand I, Cella M, Lanzavecchia A, Banchereau J. CD34+ hematopoietic progenitors from human cord blood differentiate along two independent dendritic cell pathways in response to granulocyte-macrophage colony-stimulating factor plus tumor necrosis factor alpha: II. Functional analysis. Blood. 1997; 90:1458–1470. [PubMed: 9269763]
5. Jego G, Palucka AK, Blanck JP, Chalouni C, Pascual V, Banchereau J. Plasmacytoid dendritic cells induce plasma cell differentiation through type I interferon and interleukin 6. Immunity. 2003; 19:225–234. [PubMed: 12932356]
6. Ueno H, Klechevsky E, Morita R, Aspord C, Cao T, Matsui T, Di Pucchio T, Connolly J, Fay JW, Pascual V, Palucka AK, Banchereau J. Dendritic cell subsets in health and disease. Immunol Rev. 2007; 219:118–142. [PubMed: 17850486]
7. Fernandez-Sesma A, Marukian S, Ebersole BJ, Kaminski D, Park MS, Yuen T, Sealfon SC, Garcia-Sastre A, Moran TM. Influenza virus evades innate and adaptive immunity via the NS1 protein. J Virol. 2006; 80:6295–6304. [PubMed: 16775317]
8. Yoneyama M, Kikuchi M, Natsukawa T, Shinobu N, Imaizumi T, Miyagishi M, Taira K, Akira S, Fujita T. The RNA helicase RIG-I has an essential function in double-stranded RNA-induced innate antiviral responses. Nature Immunology. 2004; 5:730–737. [PubMed: 15208624]
9. Hornung V, Ellegast J, Kim S, Brzozka K, Jung A, Kato H, Poeck H, Akira S, Conzelmann KK, Schlee M, Endres S, Hartmann G. 5'-Triphosphate RNA is the ligand for RIG-I. Science. 2006; 314:994–997. [PubMed: 17038590]
10. Pichlmair A, Schulz O, Tan CP, Naslund TI, Liljestrom P, Weber F, Reis e Sousa C. RIG-I-mediated antiviral responses to single-stranded RNA bearing 5'-phosphates. Science. 2006; 314:997–1001. [PubMed: 17038589]
11. Macagno A, Napolitani G, Lanzavecchia A, Sallusto F. Duration, combination and timing: the signal integration model of dendritic cell activation. Trends Immunol. 2007; 28:227–233. [PubMed: 17403614]
12. Murray PJ. The JAK-STAT signaling pathway: input and output integration. J Immunol. 2007; 178:2623–2629. [PubMed: 17312100]
13. Reis e Sousa C. Dendritic cells in a mature age. Nature Reviews. Immunology. 2006; 6:476–483.
14. Mellman I, Steinman RM. Dendritic cells: specialized and regulated antigen processing machines. Cell. 2001; 106:255–258. [PubMed: 11509172]
15. Coppey M, Berezhkovskii AM, Sealfon SC, Shvartsman SY. Time and length scales of autocrine signals in three dimensions. Biophys J. 2007; 93:1917–1922. [PubMed: 17720734]
16. Kato H, Sato S, Yoneyama M, Yamamoto M, Uematsu S, Matsui K, Tsujimura T, Takeda K, Fujita T, Takeuchi O, Akira S. Cell type-specific involvement of RIG-I in antiviral response. Immunity. 2005; 23:19–28. [PubMed: 16039576]
17. Park MS, Garcia-Sastre A, Cros JF, Basler CF, Palese P. Newcastle disease virus V protein is a determinant of host range restriction. J Virol. 2003; 77:9522–9532. [PubMed: 12915566]
18. Park MS, Shaw ML, Munoz-Jordan J, Cros JF, Nakaya T, Bouvier N, Palese P, Garcia-Sastre A, Basler CF. Newcastle disease virus (NDV)-based assay demonstrates interferon-antagonist activity for the NDV V protein and the Nipah virus V, W, and C proteins. J Virol. 2003; 77:1501–1511. [PubMed: 12502864]

19. Mibayashi M, Martinez-Sobrido L, Loo YM, Cardenas WB, Gale M Jr. Garcia-Sastre A. Inhibition of retinoic acid-inducible gene I-mediated induction of beta interferon by the NS1 protein of influenza A virus. J Virol. 2007; 81:514–524. [PubMed: 17079289]
20. Lopez CB, Garcia-Sastre A, Williams BR, Moran TM. Type I interferon induction pathway, but not released interferon, participates in the maturation of dendritic cells induced by negative-strand RNA viruses. J Infect Dis. 2003; 187:1126–1136. [PubMed: 12660927]
21. Yuen T, Wurmbach E, Pfeffer RL, Ebersole BJ, Sealfon SC. Accuracy and calibration of commercial oligonucleotide and custom cDNA microarrays. Nucleic Acids Res. 2002; 30:e48. [PubMed: 12000853]
22. Krutzik PO, Nolan GP. Fluorescent cell barcoding in flow cytometry allows high-throughput drug screening and signaling profiling. Nat Methods. 2006; 3:361–368. [PubMed: 16628206]
23. Perfetto SP, Ambrozak D, Nguyen R, Chattopadhyay P, Roederer M. Quality assurance for polychromatic flow cytometry. Nat Protoc. 2006; 1:1522–1530. [PubMed: 17406444]
24. Haralick RM, Shanmugan K, Dinstein I. Textural features for image classification. IEEE Transactions on Systems, Man, and Cybernetics. 1973; SMC-3:610–621.
25. Lopez CB, Fernandez-Sesma A, Czelusniak SM, Schulman JL, Moran TM. A mouse model for immunization with ex vivo virus-infected dendritic cells. Cell Immunol. 2000; 206:107–115. [PubMed: 11161442]
26. Perry AK, Chen G, Zheng D, Tang H, Cheng G. The host type I interferon response to viral and bacterial infections. Cell Res. 2005; 15:407–422. [PubMed: 15987599]
27. Randolph GJ, Beaulieu S, Pope M, Sugawara I, Hoffman L, Steinman RM, Muller WA. A physiologic function for p-glycoprotein (MDR-1) during the migration of dendritic cells from skin via afferent lymphatic vessels. Proc Natl Acad Sci U S A. 1998; 95:6924–6929. [PubMed: 9618515]
28. Bosnjak L, Miranda-Saksena M, Koelle DM, Boadle RA, Jones CA, Cunningham AL. Herpes simplex virus infection of human dendritic cells induces apoptosis and allows cross-presentation via uninfected dendritic cells. J Immunol. 2005; 174:2220–2227. [PubMed: 15699155]
29. Pollara G, Jones M, Handley ME, Rajpopat M, Kwan A, Coffin RS, Foster G, Chain B, Katz DR. Herpes simplex virus type-1-induced activation of myeloid dendritic cells: the roles of virus cell interaction and paracrine type I IFN secretion. J Immunol. 2004; 173:4108–4119. [PubMed: 15356161]
30. Palmer DR, Sun P, Celluzzi C, Bisbing J, Pang S, Sun W, Marovich MA, Burgess T. Differential effects of dengue virus on infected and bystander dendritic cells. J Virol. 2005; 79:2432–2439. [PubMed: 15681444]
31. Santini SM, Lapenta C, Logozzi M, Parlato S, Spada M, Di Pucchio T, Belardelli F. Type I interferon as a powerful adjuvant for monocyte-derived dendritic cell development and activity in vitro and in Hu-PBL-SCID mice. J Exp Med. 2000; 191:1777–1788. [PubMed: 10811870]
32. Luft T, Pang KC, Thomas E, Hertzog P, Hart DN, Trapani J, Cebon J. Type I IFNs enhance the terminal differentiation of dendritic cells. J Immunol. 1998; 161:1947–1953. [PubMed: 9712065]
33. Blanco P, Palucka AK, Gill M, Pascual V, Banchereau J. Induction of dendritic cell differentiation by IFN-alpha in systemic lupus erythematosus. Science. 2001; 294:1540–1543. [PubMed: 11711679]
34. Watanabe N, Hanabuchi S, Soumelis V, Yuan W, Ho S, de Waal Malefyt R, Liu YJ. Human thymic stromal lymphopoietin promotes dendritic cell-mediated CD4+ T cell homeostatic expansion. Nat Immunol. 2004; 5:426–434. [PubMed: 14991051]
35. Soumelis V, Reche PA, Kanzler H, Yuan W, Edward G, Homey B, Gilliet M, Ho S, Antonenko S, Lauerma A, Smith K, Gorman D, Zurawski S, Abrams J, Menon S, McClanahan T, de Waal-Malefyt Rd R, Bazan F, Kastelein RA, Liu YJ. Human epithelial cells trigger dendritic cell mediated allergic inflammation by producing TSLP. Nat Immunol. 2002; 3:673–680. [PubMed: 12055625]
36. Chomarat P, Dantin C, Bennett L, Banchereau J, Palucka AK. TNF skews monocyte differentiation from macrophages to dendritic cells. J Immunol. 2003; 171:2262–2269. [PubMed: 12928370]
37. Steinbrink K, Wolfl M, Jonuleit H, Knop J, Enk AH. Induction of tolerance by IL-10-treated dendritic cells. J Immunol. 1997; 159:4772–4780. [PubMed: 9366401]

38. Sato K, Yamashita N, Baba M, Matsuyama T. Regulatory dendritic cells protect mice from murine acute graft-versus-host disease and leukemia relapse. Immunity. 2003; 18:367–379. [PubMed: 12648454]
39. Martin-Fontecha A, Thomsen LL, Brett S, Gerard C, Lipp M, Lanzavecchia A, Sallusto F. Induced recruitment of NK cells to lymph nodes provides IFN-gamma for T(H)1 priming. Nat Immunol. 2004; 5:1260–1265. [PubMed: 15531883]
40. Mohamadzadeh M, Berard F, Essert G, Chalouni C, Pulendran B, Davoust J, Bridges G, Palucka AK, Banchereau J. Interleukin 15 skews monocyte differentiation into dendritic cells with features of Langerhans cells. J Exp Med. 2001; 194:1013–1020. [PubMed: 11581322]
41. Dubsky P, Saito H, Leogier M, Dantin C, Connolly JE, Banchereau J, Palucka AK. IL-15-induced human DC efficiently prime melanoma-specific naive CD8+ T cells to differentiate into CTL. Eur J Immunol. 2007; 37:1678–1690. [PubMed: 17492620]
42. Mattei F, Schiavoni G, Belardelli F, Tough DF. IL-15 is expressed by dendritic cells in response to type I IFN, double-stranded RNA, or lipopolysaccharide and promotes dendritic cell activation. J Immunol. 2001; 167:1179–1187. [PubMed: 11466332]
43. Janes KA, Albeck JG, Gaudet S, Sorger PK, Lauffenburger DA, Yaffe MB. A systems model of signaling identifies a molecular basis set for cytokine-induced apoptosis. Science. 2005; 310:1646–1653. [PubMed: 16339439]
44. Janes KA, Yaffe MB. Data-driven modelling of signal-transduction networks. Nat Rev Mol Cell Biol. 2006; 7:820–828. [PubMed: 17057752]
45. Miller-Jensen K, Janes KA, Brugge JS, Lauffenburger DA. Common effector processing mediates cell-specific responses to stimuli. Nature. 2007; 448:604–608. [PubMed: 17637676]
46. Hoshino K, Kaisho T, Iwabe T, Takeuchi O, Akira S. Differential involvement of IFN-beta in Toll-like receptor-stimulated dendritic cell activation. Int Immunol. 2002; 14:1225–1231. [PubMed: 12356687]
47. Honda K, Sakaguchi S, Nakajima C, Watanabe A, Yanai H, Matsumoto M, Ohteki T, Kaisho T, Takaoka A, Akira S, Seya T, Taniguchi T. Selective contribution of IFN-alpha/beta signaling to the maturation of dendritic cells induced by double-stranded RNA or viral infection. Proc Natl Acad Sci U S A. 2003; 100:10872–10877. [PubMed: 12960379]
48. Hoebe K, Janssen EM, Kim SO, Alexopoulou L, Flavell RA, Han J, Beutler B. Upregulation of costimulatory molecules induced by lipopolysaccharide and double-stranded RNA occurs by Trif-dependent and Trif-independent pathways. Nat Immunol. 2003; 4:1223–1229. [PubMed: 14625548]
49. Sporri R, Reis e Sousa C. Inflammatory mediators are insufficient for full dendritic cell activation and promote expansion of CD4+ T cell populations lacking helper function. Nat Immunol. 2005; 6:163–170. [PubMed: 15654341]
50. Brankston G, Gitterman L, Hirji Z, Lemieux C, Gardam M. Transmission of influenza A in human beings. Lancet Infectious Diseases. 2007; 7:257–265. [PubMed: 17376383]
51. Garcia-Sastre A. Identification and characterization of viral antagonists of type I interferon in negative-strand RNA viruses. Curr Top Microbiol Immunol. 2004; 283:249–280. [PubMed: 15298172]
52. Garcia-Sastre A, Biron CA. Type 1 interferons and the virus-host relationship: a lesson in detente. Science. 2006; 312:879–882. [PubMed: 16690858]
53. Alcami A. Viral mimicry of cytokines, chemokines and their receptors. Nat Rev Immunol. 2003; 3:36–50. [PubMed: 12511874]

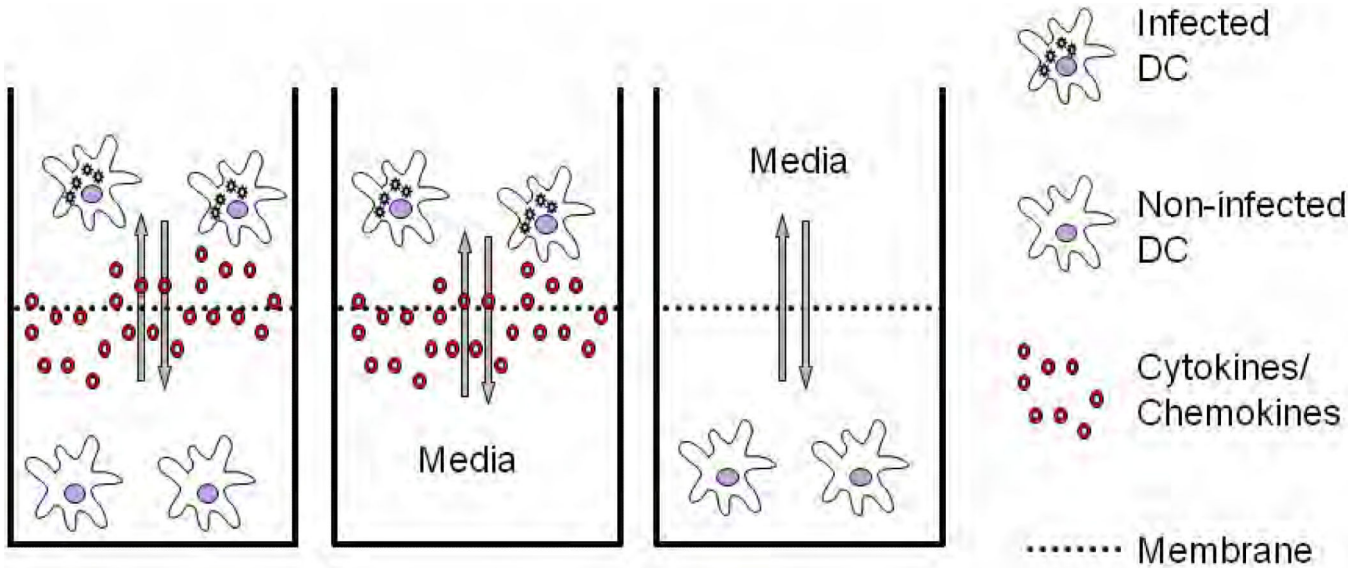

Figure 1.
Experimental setup for the generation of AVDCs.

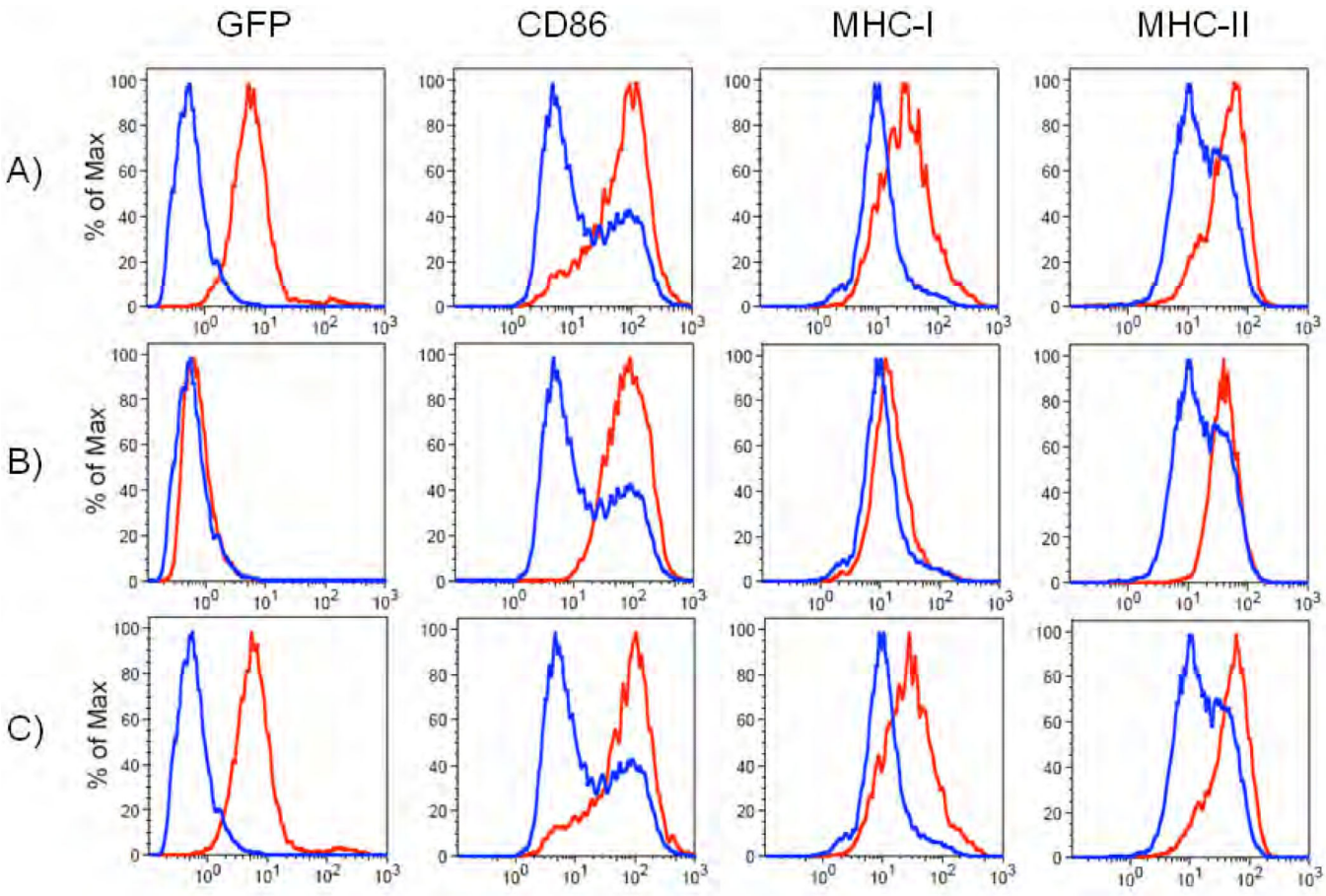

Figure 2.

Expression of viral GFP protein, and maturation markers in infected DCs, AVDCs and non infected DCs. Histograms show fluorescence intensity of cells for the viral GFP tagged protein NDV-HN and the fluochrome conjugated antibodies for CD86, HLA-ABC (MHC-I) and HLA-DR (MHC-II). Blue histogram indicates non-infected DC control. Red histograms indicate, A) Infected DCs in the trans-well system, B) AVDCs, and C) Infected DCs as positive control. The data shown are representative of three different experiments using three different donors that showed similar results.

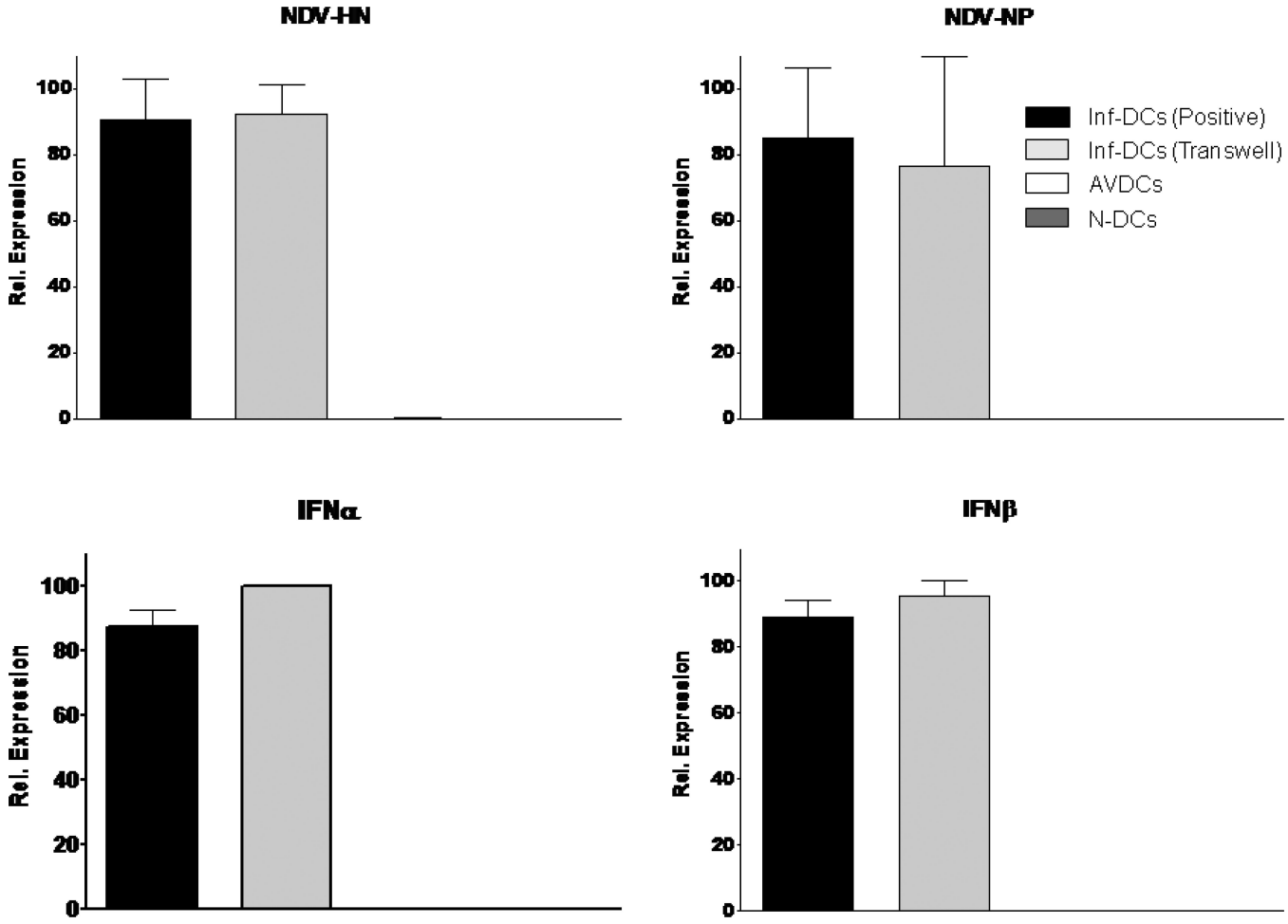

Figure 3.

Quantitative RT-PCR of RNA expression for virus and type I IFN genes in infected control DCs (Inf-DC), infected DCs from the trans-well cultures, AVDCs and non-infected naïve DCs (N-DC) genes to viral infection. The results shown are averages of three independent experiments performed using different donors.

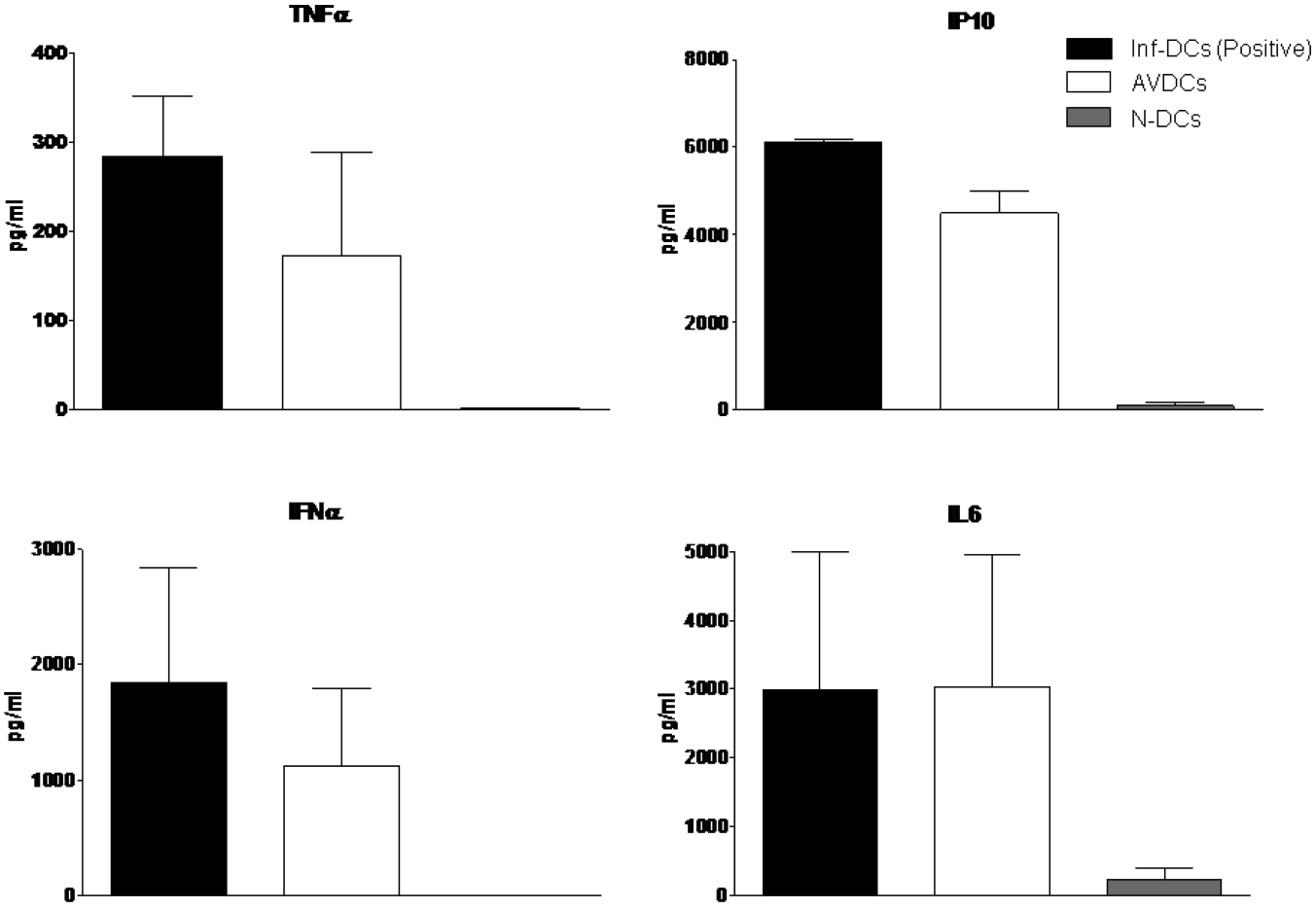

Figure 4.

Multiplex ELISA for IL6, IP10, TNFα and IFNα levels in supernatants from the chambers containing infected DCs, AVDCs and non-infected naïve DCs (N-DC) genes to viral infection, all in the trans-well systems. The results shown are averages of three independent experiments performed using different donors.

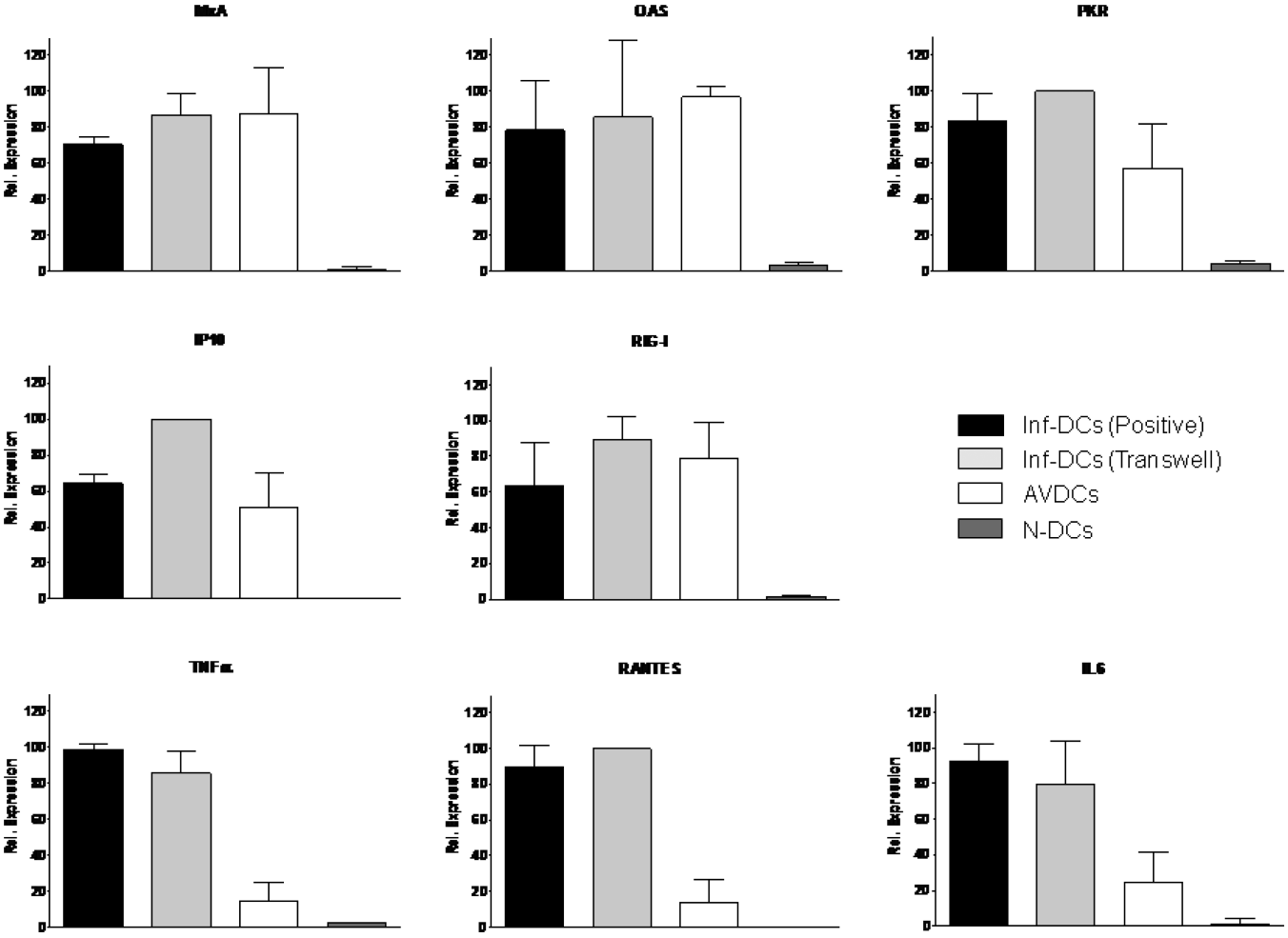

Figure 5.

Quantitative RT-PCR of antiviral and inflammatory gene expression in infected control DCs (Inf-DC), infected DCs from the trans-well cultures, AVDCs and non-infected naïve DCs (N-DC) genes to viral infection. The results shown are averages of three independent experiments performed using different donors.

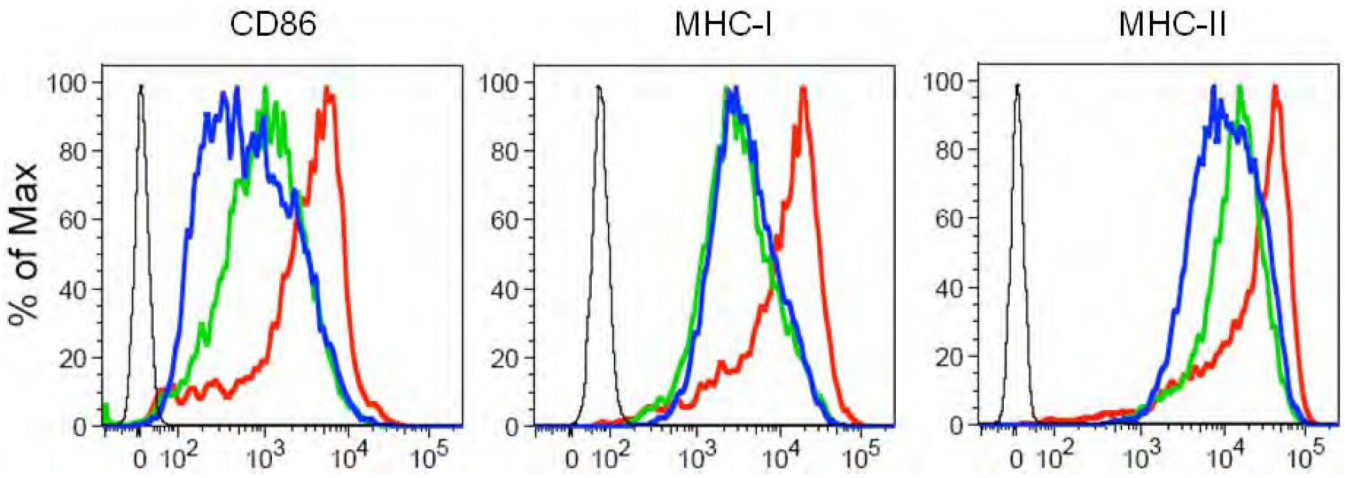

Figure 6.

Flow cytometry analysis studying the involvement of IFNβ signaling in the generation of AVDCs. CD86, MHC-I and MHC-II were assayed and the results are shown in the different columns. Blue indicates treatment of naïve DCs with IFNβ cytokine, green indicates AVDCs and red infected DCs as control The data shown are representative of three different experiments using three different donors that showed similar results.

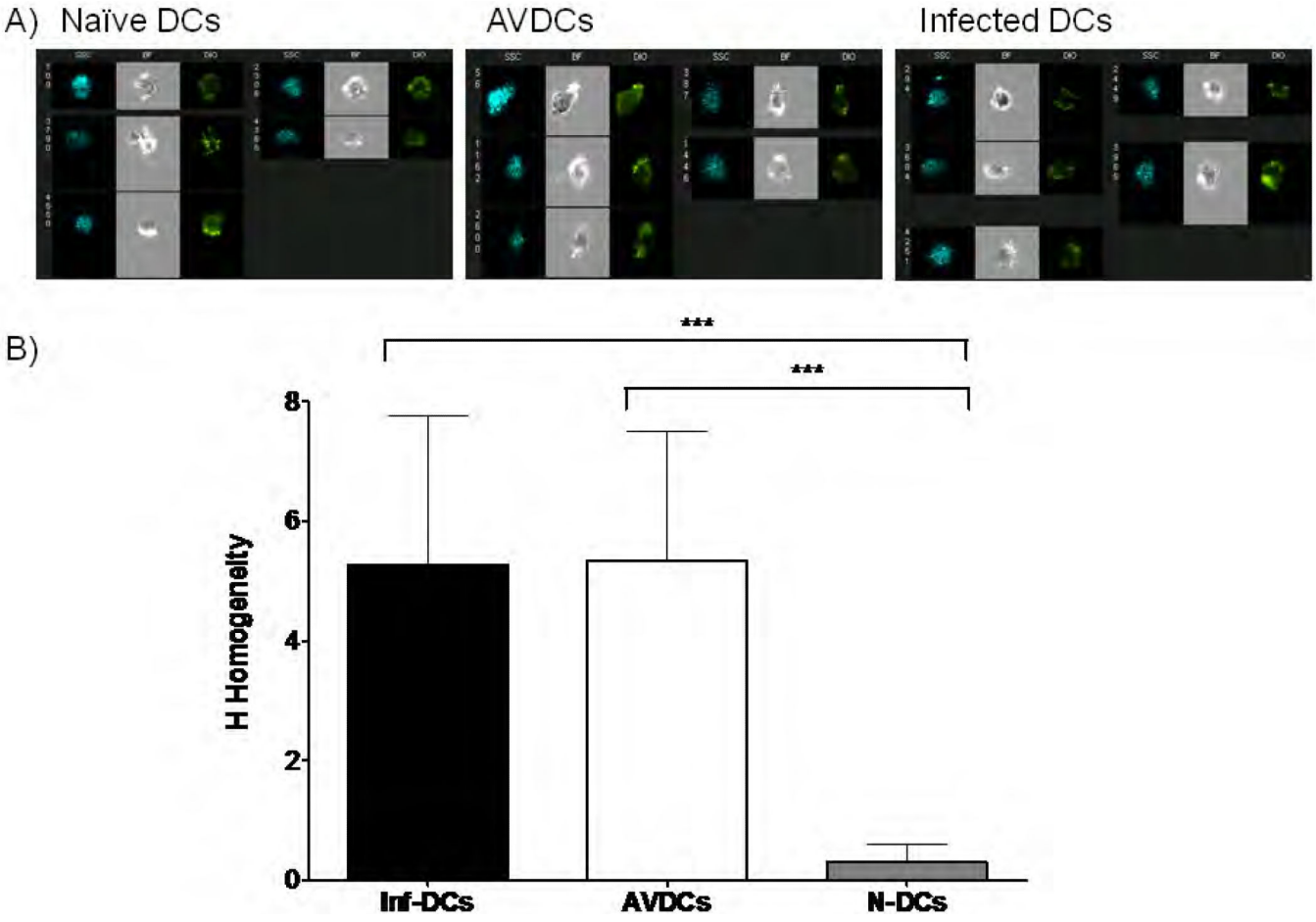

Figure 7.

Homogeneity test to show differences in morphological shapes. A) Representative pictures of naïve DCs, AVDCs and infected control DCs captured using an imaging flow cytometry. B) Histogram of the homogeneity value of naïve DCs, AVDCs and infected DCs. *** p<. 0001 by Mann Whitney test in comparison with naïve DCs. The results shown are averages of three independent experiments performed using different donors.

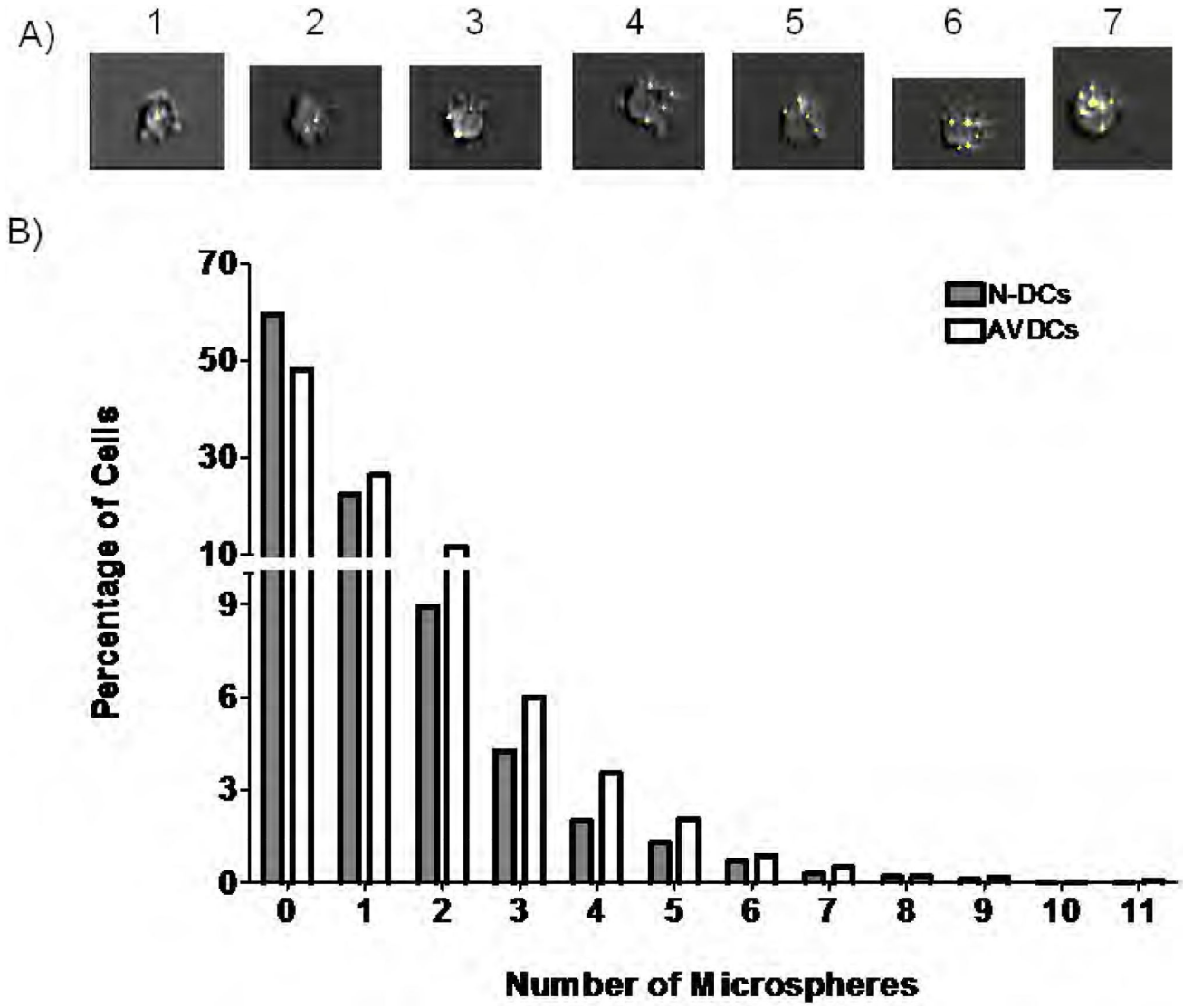

Figure 8.

Phagocytosis of Microspheres. A) Representative images showing examples of cells containing between one and seven beads imaged using enhanced depth of field-equipped imaging flow cytometry. B) Distribution of number of microspheres counted in naïve DCs (n=2000) and AVDCs (n=2700). The distributions are statistically different ($p<10^{-13}$). The data shown are representative of three different experiments using cells from three different donors that showed similar results.

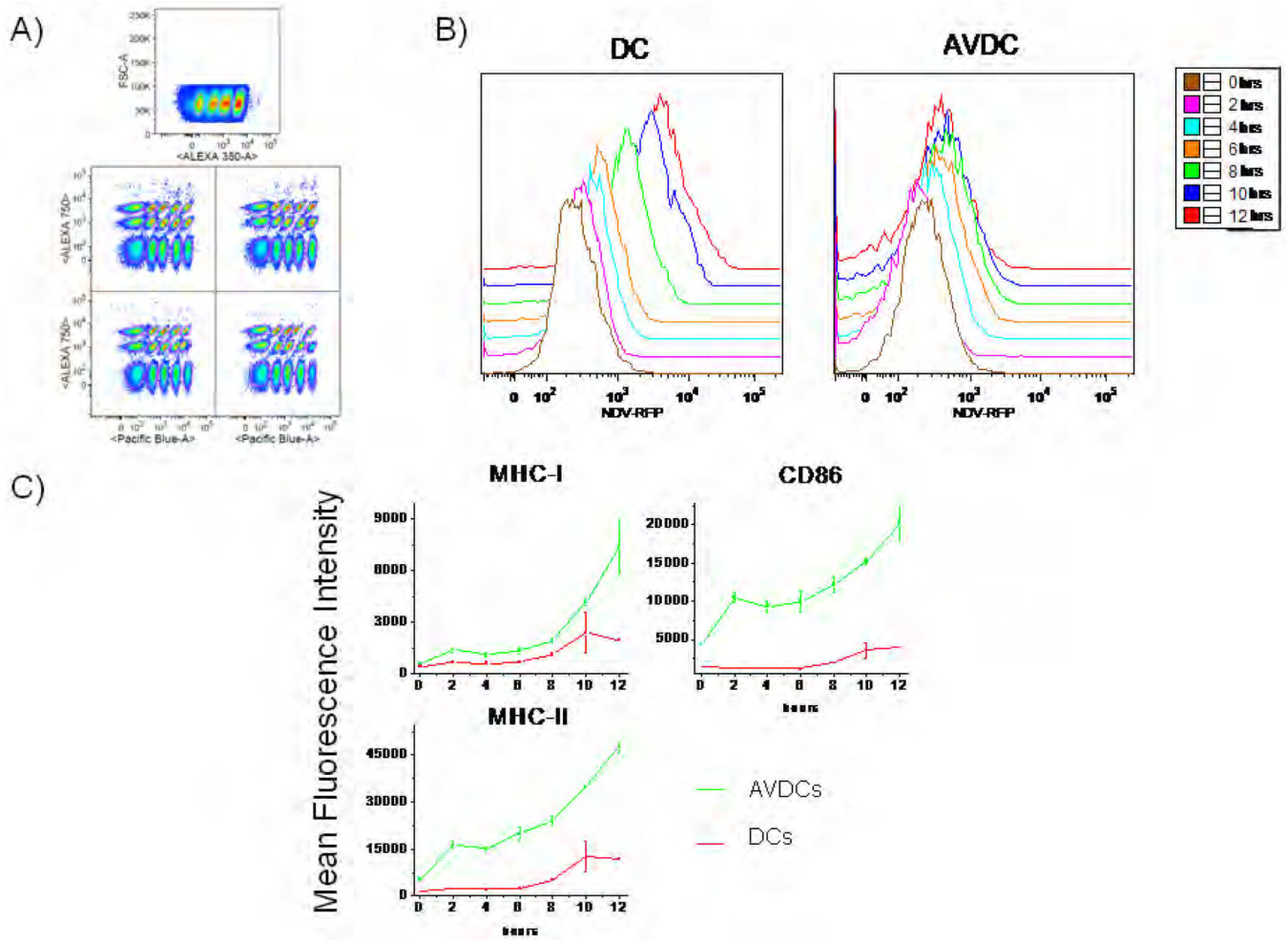

Figure 9.

AVDCs resist viral infection. A) Barcoding for flow cytometry analysis. Cells were stained with different combinations of 0, 0.3, 1, 4 or 15 μg/ml Pacific Blue–NHS, 0, 1.25, 5 or 20 μg/ml Alexa 350–NHS and 0, 4 or 20 μg/ml Alexa 750–NHS to enable 60 different conditions in one FACS run. B) Time course results for NDV-RFP expression following infection in naïve DC and AVDC. C) Time course for expression of MHC-I, MHC-II and CD86 surface markers in the same cells studied in A and B. The results shown are representative of two independent experiments using cells from different donors.

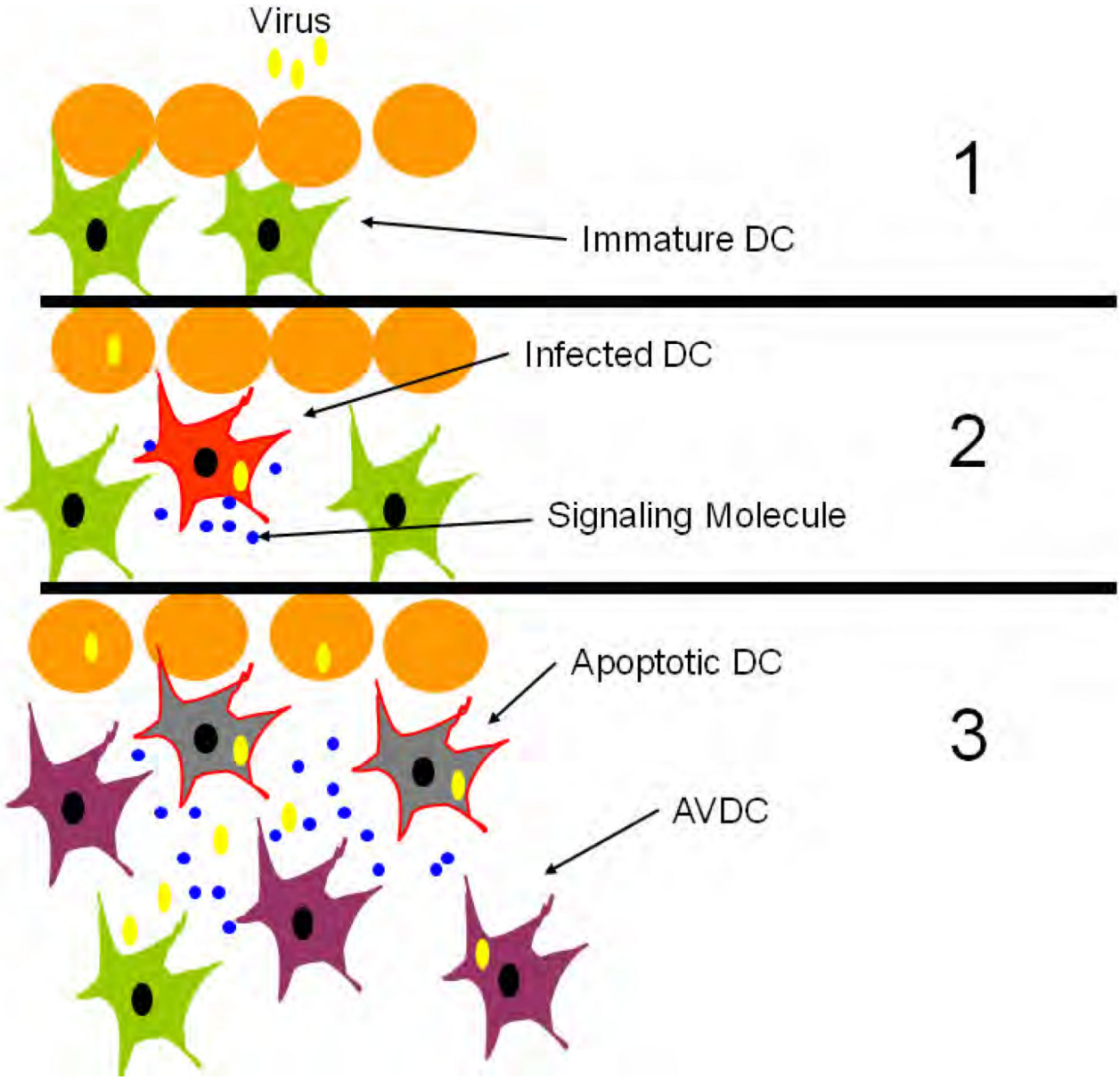

Figure 10.
Schematic of the possible role of AVDCs in developing adaptive immunity. The paracrine signals released by DCs that are first infected by virus generate AVDCs that are primed to resist virus and to develop into antigen presenting cells.